Chapter 15
Electrical Conductivity Depth Functions for Delineating Paleosols

Glenn Borchardt

Abstract Soil weathering and leaching lead to increased salt concentrations at the wetting front in soils of semiarid and Mediterranean climates. Burial of silty alluvial fan deposits may preserve these salt signatures in paleosols, with the base of each solum being delineated by high electrical conductivity. The buried layer must be thick enough to prevent destruction of the initial signature via leaching. The identification of alluvial strata as paleosol horizons helps to confirm age estimates derived from standard soil descriptions. Several examples illustrate the use of conductivity in delineating late Quaternary soils and paleosols. A soil profile along the Hayward fault had a soil underlain by three paleosols instead of the four paleosols as was first assumed by visual examination. Estimates of soil and paleosol ages were sufficient to assure that no surface fault rupture had occurred during the last 24,000 years. Background conductivity was about 200 μS/cm, while maxima for the soil and three paleosols were 560, 580, 630, and 590 μS/cm, respectively. It was concluded that field electrical conductivity measurements can be used to delineate paleosols.

Keywords Pedochronology · Faulting · Tectonics · Electrical conductivity · Depth functions

15.1 Introduction

Soil weathering and leaching lead to increased salt concentrations at the wetting front in soils. In uniform, fine-textured soil measurements of electrical conductivity (EC) within soil solutions may indicate the extent of this process (Frinkl 1979; Pozdnyakova 1999; Golovko et al. 2007; Son et al. 2010). However, due to the great solubility of salts released from minerals, concentrations typically are low and ephemeral, particularly in soils of the humid regions.

G. Borchardt (✉)
Soil Tectonics, Berkeley, CA, USA
e-mail: gborchardt@gmail.com

A.E. Hartemink and B. Minasny (eds.), *Digital Soil Morphometrics*,
Progress in Soil Science, DOI 10.1007/978-3-319-28295-4_15

In California, EC measurements have been used to aid in pedochronology (soil dating), which we use in assessing the age of fault movement. State law prohibits most construction on earthquake faults that had surface fault rupture (SFR) during the Holocene (Bryant and Hart 2007). To gauge the hazard, geologists excavate 3 to 6-m-deep trenches perpendicular to suspect fault traces across potential building sites. As a pedochronologist, I estimate the ages of soils and any associated faulting exposed in these trenches. Although the modern soil in many of the trenches may have begun developing less than the required 11,000 years, we sometimes find paleosols beneath them. EC measurements may help to confirm that such soils indeed are paleosols. Soil development durations are estimated from peak heights in combination with other age-related characteristics such as color, B horizon thickness and structure, clay film development, and calcite stage.

15.2 Materials and Methods

We generally describe soil profiles that represent the oldest, most complete record of soil development in the trench excavations that geologists use to evaluate the presence of hazardous faults. If a fault is discovered, this may necessitate sampling, measuring, and describing soils about a meter on either side of the suspect fault. Vertical channel samples of each horizon are obtained as representative.

In the laboratory, EC and pH are measured after representative subsamples are mixed with an equal amount of water by weight. EC measurements can be performed in the field or laboratory with a handheld meter (Fig. 15.1). EC values could be used to produce in situ analog depth functions that could help in delineating soil horizons. However, EC and its inverse, electrical resistivity are influenced by the amount of moisture present (Ozcep et al. 2010). The water to soil ratio must be controlled. Dry soils do not yield EC measurements (Brevik et al. 2006), as demonstrated by the Phoenix Mars Lander, which failed to get a response even though there was ice within 5 cm of the probe (Zent et al. 2009). Coarse soils and sediments generally do not trap salts. Although this low EC response may aid in the identification of sand and gravel lenses (Fig. 15.2), it may also prevent the development of an EC peak that would indicate the extent of the wetting front.

15.3 Results

15.3.1 Holocene Soil (10 ka)

Although soil weathering was minimal in California during the Holocene, we can detect its occurrence by performing EC measurements. Depth functions for EC indicate that a particular soil has received sufficient precipitation to induce soil

Fig. 15.1 Simple, typical handheld electrical conductivity meter

formation. Leaching from the A horizon generally removes salts released from soil minerals. These salts move to the wetting front. A typical soil has received rainfall with carbonic acid formed from carbon dioxide in the atmosphere. This naturally acidifies and decalcifies the soil, with surface horizons countering that trend as they accumulate Ca-laden vegetative matter (Fig. 15.3). EC measurements follow a similar pattern (Fig. 15.4). The soil pH was lowest at the 140 cm depth, which also was the depth that the EC began to increase. The upper 33 cm of the soil was imported artificial fill.

15.3.2 Pleistocene–Holocene Transition

The climate change from humid to subhumid that occurred as a result of the Pleistocene–Holocene transition in northern California has provided valuable information for pedochronology. Holocene soils tend to be about a meter thick, while soils formed during the Pleistocene can be up to several meters thick. When there is associated colluvial or alluvial deposition, EC depth functions sometimes reflect both soil moisture regimes (Fig. 15.5).

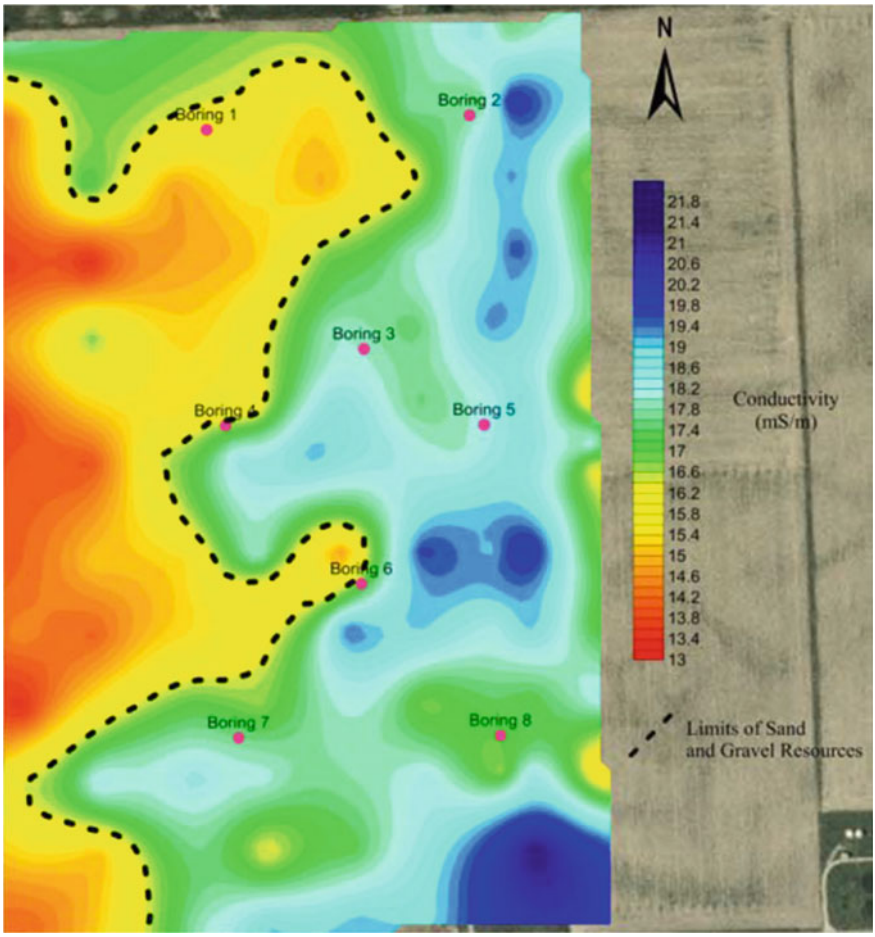

Fig. 15.2 EC measurements showing the effect of particle size. Reddish areas have low EC in the sand and gravel areas (Mundell and Associates, Inc. 2015)

Micropedology sometimes can be used to confirm the transition from one climate to another or, alternatively, the effect of alluvial deposition or erosion. For instance, peds that were coated with clay films during the Pleistocene can be subsequently coated with soluble salts that demonstrate that the wetting front has risen in the profile. Figure 15.6 shows gypsum coating a ped formed when the landscape was subject to much greater water percolation.

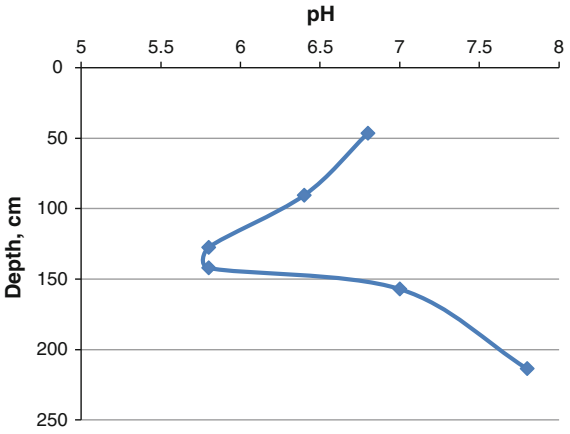

Fig. 15.3 Depth function for pH in Soil Profile No. 1 in Trench EFT-1 on Toro Vista Court (10 ka/70 ka; MAP = 551 mm/year) (Borchardt 2007, Fig. 2). Note that the upper 33 cm of this profile was artificial fill

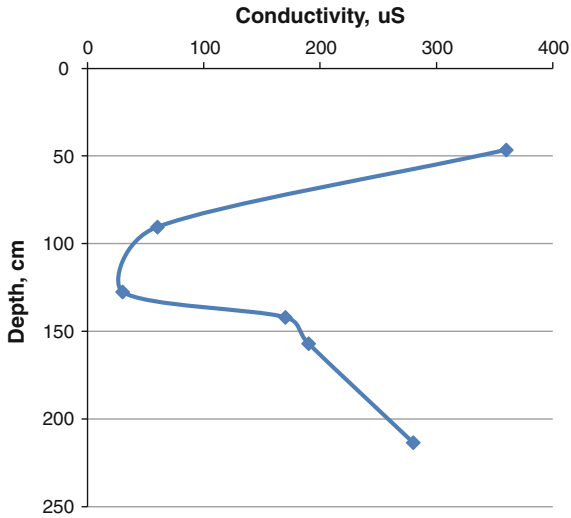

Fig. 15.4 Depth function for EC in Soil Profile No. 1 in Trench EFT-1 on Toro Vista Court (10 ka/70 ka; MAP 551 mm/year) (Borchardt 2007, Fig. 3). Note that the upper 33 cm of this profile was artificial fill

15.3.3 Sangamon Soil (122 ka)

Relict paleosols considered to be Sangamon age (the last time sea level was higher than at present, Chen et al. 1991) sometimes exist on stable surfaces devoid of significant degradation or aggradation during the Pleistocene/Holocene transition. Salts are left behind as the wetting front gradually retreats toward the surface when the climate becomes increasingly dry (Fig. 15.7). Such uniform behavior is dependent on a relatively uniform fine soil texture. Salt concentrations in coarse horizons tend to be low due to their low water holding capacity and high permeability (Figs. 15.2 and 15.8). In the Sangamon paleosol, the upper two silt loam horizons have been leached extensively during the Holocene (Fig. 15.7), while the

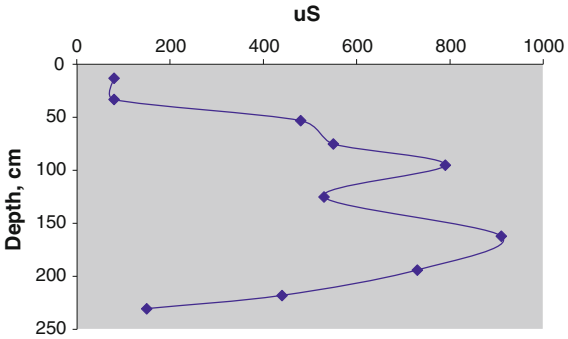

Fig. 15.5 Depth function for EC in Soil Profile No. 3 at the Lakes at Fountain Grove, Santa Rosa, CA. The two high EC peaks may represent two distinct phases of soil development, with paleosol development during the Pleistocene being interrupted by the colluviation that contributed parent material for the modern soil (10 ka/80 ka; MAP 1067 mm/year) (Borchardt 2003, Fig. 6)

Fig. 15.6 Close-up of clay-coated ped face surrounded by gypsum in the Etyb1 horizon of a paleosol near the Calaveras fault. The clay films were deposited first and the gypsum second. View SE (16 ka; MAP 578 mm/year) (Borchardt 2008, Fig. 5)

underlying 2-m-thick silty clay Bt horizon that formed during the Pleistocene remains preserved beneath the E horizon (Fig. 15.9).

California state law prohibits construction on faults having had surface fault rupture during the Holocene for residential housing developments. Even though this soil was much older than that, it had experienced several fault offsets since 122 ka. These totaled about 1 m and probably were the results of several earthquakes. During that period, the subparallel San Andreas fault about 6 km to the east had undergone 3000 m of lateral offset. The faults at this site had negligible activity. In addition, there was no offset of the surface topography, as is generally the case with hazardous faults. The analysis of the SFR hazard at the site indicated that up to

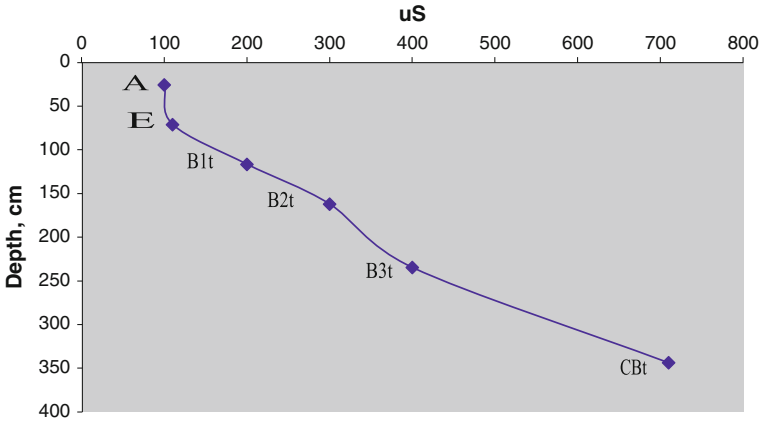

Fig. 15.7 Depth function for EC in a Pleistocene soil at Paradise Valley, Bolinas, California (122 ka; MAP = 914 mm/year) (Borchardt 2005, Fig. 2)

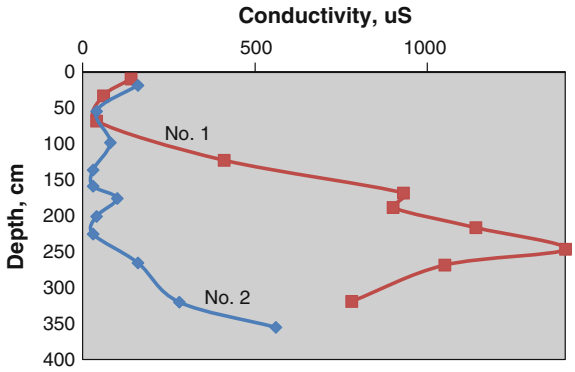

Fig. 15.8 Depth function for EC in Soil Profile Nos. 1 and 2 at Alamo, California. The high EC beneath the 130 cm depth in Soil Profile No. 1 reflects the presence of high amounts of gypsum beneath the present-day wetting front. The gravelly nature of Soil Profile No. 2 allows clays and salts to penetrate to much greater depths than they do in the silt of Soil Profile No. 1 (22 ka; MAP = 578 mm/year) (Borchardt 2008, Fig. 9)

24 cm of vertical and horizontal offset could occur in a single event (Dwyer et al. 2010). We selected 1.2 m as the maximum possible horizontal offset, which would be 20 % of what occurred on the San Andreas in 1906 (Lawson 1908; Hoexter 1992).

Fig. 15.9 Pleistocene soil at Bolinas showing the E horizon overlying the yellowish brown Bt horizon (122 ka; MAP = 914 mm) (Borchardt 2005, Fig. 3)

15.3.4 Multiple Paleosols in Young Alluvium (24 ka)

EC depth functions are useful in detecting and confirming the presence of paleosols in young alluvial fans. A change in salt concentration may convey age-related information. At a prospective building site on the southwest side of the Hayward fault, EC measurements indicated that there was a Holocene soil underlain by three short-lived paleosols (Fig. 15.10). During initial description of this soil profile, an additional paleosol was assumed when viewing the faunal bone in the section (Fig. 15.11). Bones, like most charcoal specimens, are often found at the surfaces of paleosols, similar to lag deposits. In this soil, however, a bone was in the midst of a weak, Bt horizon, which was one reason it had survived the relatively short period

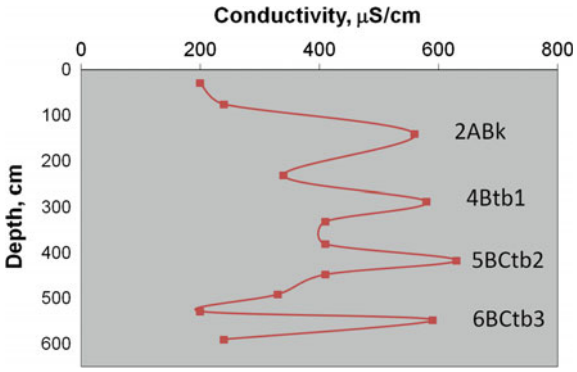

Fig. 15.10 Depth function for EC showing maxima for the modern soil and three underlying paleosols along the Hayward fault (24 ka; MAP = 640 mm/year) (Borchardt 2015, Fig. 7)

Fig. 15.11 View of the 5B2tb2 horizon from Soil Profile No. 3 showing a bone fragment at the 405 cm depth (Borchardt 2015, Fig. 4)

Table 15.1 Comparison of pedochronological estimates derived from the profile description with estimates derived from the relative areas of EC peaks

Horizon	Duration of soil development (t_d) (ky)	
	Borchardt (2015)	EC peak area
2ABk	11.0[a]	10.0[b]
4Btb1	4.0	4.9
5BCtb2	5.0	3.5
6BCtb3	4.0	5.4
Profile t_o, ka	24.0	23.8

[a]Pedochronological estimates based on available information. All ages should be considered subject to ±50 % variation unless otherwise indicated (Borchardt 1992)
[b]Peak areas were calculated by multiplying half the height of the EC peak (μS/cm) times the width of the base of the peak (cm)
t_o = date when soil formation or aggradation began, ka
t_b = date when soil or strata were buried, ka
t_d = duration of soil development or aggradation, ky

(5 ky) of weathering. Background EC was about 200 μS/cm, while maxima for the soil and three paleosols were 560, 580, 630, and 590 μS/cm, respectively (Fig. 15.10). These results reflect the relatively high average deposition rate (0.24 mm/year) necessary to safeguard EC maxima from dissolution by percolation from overlying deposits.

There is a possibility that the actual quantity of soluble salt preserved in these soils and paleosols is correlative with the amount of time each was exposed to pedogenesis. For instance, in the above example, I calculated the areas of the four EC peaks after performing the usual qualitative estimates of development durations (Table 15.1). The two methods appear to be somewhat correlative, showing that quantitative measurements of soluble salts, along with more detailed EC measurements, may have promise in future pedochronological studies.

15.4 Conclusions

These results highlight the use of EC measurements in pedochronology and the estimation of soil age. Salts dissolved from weathering minerals percolate in soil solutions and are generally deposited at the wetting front. This mostly occurs in Mediterranean and semiarid to arid climates where salts are not leached from fine-textured soils. With sufficient aggradation, salt accumulations can be preserved, providing evidence for previous soil formation in the form of paleosols. Unlike pH measurements, changes in EC may appear minuscule, but they can be important indicators of pedogenesis. EC measurements can help in descriptions of paleosols that provide valuable information on previous landscapes and climates. Salt concentrations as indicators of soil weathering should receive more attention than they are normally given, particularly in areas subject to semiarid and Mediterranean climates, where salts tend to tarry on their way to the sea.

Acknowledgments I thank M.J. Dwyer, Certified Engineering Geologist, Santa Rosa, California, and Alfred Hartemink, University of Wisconsin-Madison, Department of Soil Science, for many helpful suggestions that improved the manuscript.

References

Borchardt G (1992) Pedochronology along the Hayward fault. In: Borchardt G, Hirschfeld SE, Lienkaemper JJ, McClellan P, Williams PL, Wong IG (eds) Proceedings of the second conference on earthquake hazards in the Eastern San Francisco Bay Area, 25–29 March 1992, Hayward, California, California Department of Conservation, Division of Mines and Geology Special Publication 113, pp 111–117

Borchardt G (2003) Pedochronological report for The Lakes at Fountain Grove, Santa Rosa, California, Unpublished consulting report prepared for RGH Geotechnical and Environmental Consultants, Santa Rosa, California, RGH Project No. 1780.02.08.1, Berkeley, California, Soil Tectonics, A-1 to A-16

Borchardt G (2005) Pedochronological report for the Osterweis Property, Paradise Valley Road, Bolinas, California, in Samrad, LA, Dwyer, MJ (eds) Fault trench investigation: Osterweis Property, APN 188-140-11 (5.8 Acres) & APN 188-120-31 (66 Acres), Paradise Valley Road, Bolinas, California: Unpublished consulting report prepared for Mr. John Osterweis, Osterweis Capital Management, San Francisco, California, Miller Pacific Engineering Group Project No. 1147.02: Novato, California, Miller Pacific Engineering Group, C-1 to C-27

Borchardt G (2007) Pedochronological report for 2785 Toro Vista Court, Morgan Hill, California, in Connelly, SF (ed) Fault investigation: APN 817-70-007, 2875 Toro Vista Court, Morgan Hill, California: Unpublished consulting report prepared for Mr. Tony Duong, Milpitas, California, Project #0722: San Jose, California, Steven F. Connelly, C.E.G., A-1 to A-22

Borchardt G (2008) Pedochronological report for the Gordon Ball property, Camille Avenue, Alamo, California, Unpublished consulting report prepared for ENGEO, Inc., San Ramon, California, Project No. 8442.000.001, Berkeley, California, Soil Tectonics, A-1 to A-31

Borchardt G (2015) Pedochronological report for the southeast parking lot at Camp Sweeney, San Leandro, California, Unpublished consulting report for Kleinfelder, Inc., Santa Rosa, California, Berkeley, CA, Soil Tectonics, A-1 to A-33

Brevik EC, Fenton TE, Lazari A (2006) Soil electrical conductivity as a function of soil water content and implications for soil mapping. Precis Agric 7(6):393–404. doi:10.1007/s11119-006-9021-x

Bryant WA, Hart EW (2007) Fault-rupture hazard zones in California: Alquist-Priolo Earthquake Fault Zoning Act with index to Earthquake Fault Zones maps, California Geological Survey Special Publication 42, 41 p

Chen JH, Curran HA, White B, Wasserburg GJ (1991) Precise chronology of the last interglacial period: ^{234}U-^{230}Th data from fossil coral reefs in the Bahamas. Geol Soc Am Bull 103:82–97

Dwyer MJ, Samrad LA, Borchardt G, Pappas B (2010) Construction on secondary traces of the San Andreas fault at Bolinas. AEG News 53:22–25

Frinkl Jr CW (1979) Electrical conductivity. In: Fairbridge RW, Frinkl Jr CW (eds) The encyclopedia of soil science, Part 1. Physics, chemistry, biology, fertility, and technology. Dowden Hutchinson & Ross, Stroudsbug, PA, pp 97–99

Golovko L, Pozdnyakov AI (2007) Electrical geophysical methods in agriculture. In: Proceedings of the 4th international symposium on intelligent information technology in agriculture (ISIITA), 26–29 Oct 2007, Beijing, China, China National Engineering Research Center for Information Technology in Agriculture, pp 457–471

Hoexter DF (1992) Potential for triggered slip on secondary faults in the East Bay: implications for the planning process. In: Borchardt G, Hirschfeld SE, Lienkaemper JJ, McClellan P, Williams PL, Wong IG (eds) Proceedings of the second conference on earthquake hazards in

the Eastern San Francisco Bay Area: California Department of Conservation, Division of Mines and Geology Special Publication 113, pp 153–158

Lawson AC (ed) (1908) Report of the State Earthquake Investigation Commission: Washington, DC, Carnegie Institute of Washington, 2 vol, vol 1, 451 p

Mundell & Associates, Inc. (2015) Conductivity mapping to locate sand and gravel resources. Access date: 25 April 2015. http://0101.nccdn.net/1_5/207/368/181/Conductivity-Mapping-to-Locate-Sand-and-Gravel-Resources.pdf

Ozcep F, Yıldırım E, Tezel O, Asci M, Karabulut S (2010) Correlation between electrical resistivity and soil-water content based artificial intelligent techniques. Int J Phys Sci 5(1):47–56. http://www.academicjournals.org/journal/IJPS/article-abstract/F30B4EB22327

Pozdnyakova L (1999) Electrical properties of soils. PhD thesis, Laramie, WY, University of Wyoming, 138 p

Son Y, Oh M, Lee S (2010) Estimation of soil weathering degree using electrical resistivity. Environ Earth Sci 59:1319–1326

Zent AP, Hecht MH, Cobos DR, Campbell GS, Campbell CS, Cardell G, Foote MC, Wood SE, Mehta M (2009) Thermal and electrical conductivity probe (TECP) for Phoenix. J Geophys Res Planets 114(E3):E00A27